Cell and Tissue Research (2019) 378:411–425
https://doi.org/10.1007/s00441-019-03060-4

REGULAR ARTICLE

Observations on the retina and 'optical fold' of a mesopelagic sabretooth fish, *Evermanella balbo*

H.-J. Wagner[1] · J. C. Partridge[2] · R. H. Douglas[3]

Received: 18 March 2019 / Accepted: 16 June 2019 / Published online: 5 July 2019

Abstract

The 'optical fold' of *Evermanella balbo* covers the ventro-lateral cornea and is presumed to capture illumination that would otherwise remain undetected by the tubular eye of this mesopelagic teleost. It contains alternating bands of cellular and acellular material, running approximately perpendicular to the lateral surface of the eye. Only parts of this lamellar body lie within the eyelid-like structure. The cellular lamellae are 2–2.5 μm thick centrally and composed of fibroblast-like cells. The extracellular bands (4.5–5 μm thick) contain regular arrays of collagen fibrils, with layers of thin fibrils sandwiching a region of thicker fibrils. The thin fibrils are organised in alternating sheets where fibrils, although all parallel, change their orientation by 90° between each sheet. All thick fibrils are oriented parallel to the lateral surface of the 'optical fold'. In the main retina, small bundles of rod inner/outer segments are separated by the processes of the retinal pigment epithelium (rpe) laterally. Centrally, the length of tightly packed rods increases, but rpe processes no longer divide them into bundles. Medially, rod length increases further, but packing is less dense. The accessory retina is significantly thinner, and less well-developed than the main retina. Ventrally, the rods show no regular arrangement and are not grouped. Dorsally, however, rods are arranged into bundles, separated by melanosome-filled rpe processes. The thickness of the retina increases as it approaches the crystalline lens. It is on this dorsal accessory retina that light traversing the 'optical fold' most likely falls, facilitating the detection of moving objects in the ventro-lateral field of view.

Keywords Retina · Deep-sea · 'Optical fold' · Tubular eye · Grouped photoreceptors

Introduction

The deep-sea is a visually very challenging environment; not only does the level of sunlight decrease with depth, so that none can be perceived by even the most sensitive fish in the clearest waters below 1000 m (Denton 1990), the spectral content of residual sunlight also decreases to only a narrow window around 470–490 nm at depth. The other source of illumination in the deep-sea, the bioluminescence produced by the majority of animals living here, is like the remaining sunlight, similarly dim and spectrally restricted. The eyes of deep-sea fish therefore have numerous adaptations to maximise sensitivity, including enlarged pupils, visual pigments with a high absorption coefficient spectrally tuned to the available illumination, reflective tapeta and retinae usually containing only rods which either have very long outer segments or several banks of 'normally sized' rods linked to very few ganglion cells (Locket 1977; Douglas et al. 1998, 2003; Wagner et al. 1998; Warrant and Locket 2004; Douglas and Partridge 2011).

Although most species of deep-sea fish have conventional lateral, near spherical, eyes, 13 genera of mesopelagic fish have upward-pointing tubular eyes, whose large lens under a dome-shaped cornea produces a well-focussed image on a complex main retina lining the base of the tube (Franz 1907; Brauer 1908; Munk 1966; Locket 1977; Collin et al. 1997). The medial wall of the tube is lined with a more rudimentary retina, which also extends onto part of the rostral and caudal surfaces. This accessory retina is too close to the lens for the lens alone to produce a focussed image. In three genera (*Stylephorus*, *Winteria* and *Gigantura*), similar eyes are

✉ H.-J. Wagner
hjwagner@anatu.uni-tuebingen.de

[1] Anatomisches Institut der Universität Tűbingen, Ősterbergstrasse 3, 72074 Tűbingen, Germany

[2] The Oceans Institute, The University of Western Australia, Perth, WA 6009, Australia

[3] Division of Optometry & Visual Science, City, University of London, Northampton Square, London EC1V 0HB, UK

normally directed rostrally, but these animals may position themselves in the water column so that the eyes are still aimed towards the water's surface. Such tubular eyes develop from the more 'normally' positioned, approximately spherical, lateral eyes of younger animals (Contino 1939).

Upwardly directed tubular eyes increase the animal's sensitivity to the dim downwelling residual sunlight by providing an eye that has a low f-number and a large pupil, yet that can still be accommodated by the relatively small bodies of these animals. The large binocular overlap of such eyes will further enhance sensitivity (Weale 1955; Warrant and Locket 2004) and possibly provide a cue to nearby object distance. At night, such eyes will provide a bright retinal image of isolated bioluminescent flashes. In the daytime, they will also aid in the detection of dark objects seen from below, as these will appear as dark silhouettes against the residual sunlight.

Tubular eyes will, however, only gather high quality images from less than 50° of the visual space directly above the animal (Warrant and Locket 2004). Although sufficient to detect downwelling sunlight, the relatively small field of view will prevent the detection of much of the bioluminescence which occurs all around an animal (Herring 1990; Widder 1999; Haddock et al. 2010). This is clearly disadvantageous, as bioluminescence is almost certainly the dominant visual stimulus in deeper water during the day and at all depths at night (Turner et al. 2009). Thus, animals with simple dorsally directed tubular eyes will be unaware of the bioluminescence produced by animals positioned laterally or ventrally which may signal the presence of either a potential mate, a prey item or a predator.

Unsurprisingly, several species of mesopelagic fish with tubular eyes have developed devices to counter the shortcomings of this limited visual field. Among these are diverticula that extend the visual field laterally and ventrally. These range from simple retina-containing outpouchings, usually of the lateral ocular wall, in *Opisthoproctus*, *Winteria*, *Gigantura* and *Stylephorus* (Brauer 1908; Munk 1966; Locket 1977; Collin et al. 1997), which presumably do little more than sense unfocussed light, to more complex 'secondary eyes' producing better focussed images using either reflective (*Dolichopteryx longipes*-Wagner et al. 2009; *Rhynchohyalus natalensis*-Partridge et al. 2014) or refractive (*Bathylychnops exilis*-Pearcy et al. 1965) optics. The limited visual fields of the normally dorsally directed eyes of at least some barreleyed fish can be further extended by rotating their tubular eye in a forward direction (*Macropinna microstoma*-Robison and Reisenbichler 2008).

It seems likely that the visual fields of the tubular eyes of two families of aulopiform fish, the Evermanellidae and the Scopelarchidae, are also extended, not by retinal diverticula, but by lamellar structures latero-ventral to the lens and cornea (Brauer 1902, 1908; Munk 1966; Locket 1977, 2000) which channel lateral and ventral illumination into the eye. Although the structure of these 'lens pads' (Scopelarchidae) and 'optical folds' (Evermanellidae) is only partially resolved, it is clear that, although their morphology is superficially similar, there are some significant differences in structural detail, origin and potentially function (Locket 1977).

As a first step towards better understanding these enigmatic devices, we describe the anatomy of the 'optical fold' of *Evermanella balbo* (Fig. 1a), a widespread bathypelagic sabretooth fish, that usually lives at depths between 400 and 1000 m. Although the structure of this presumed device for extending the visual field laterally and ventrally has been studied before (Brauer 1908; Locket 1977), these previous descriptions are incomplete and in part erroneous. We also describe the structure of the other parts of the tubular eye of this species, including both the main and accessory retinae. Although the mechanism by which the 'optical fold' functions remains to be resolved, we hope a complete description of the eye of *E. balbo* will make the necessary optical modelling possible.

Methods

A single *E. balbo* specimen (SL 98 mm) was caught in the South Atlantic Ocean off Namibia (23° 6.09′ S, 8° 32.43′ E) using a Tucker trawl with a 4 m × 3 m opening during cruise 234-1 of the FS Sonne on the 27th of June 2014 at a depth between 500 and 800 m. After recovery of the dead fish from the net, it was transferred immediately to cold seawater (4 °C). Following identification, the fish was photographed before fixation in 4% formalin in seawater for 15 min. The head of the animal was then removed and halved medio-sagittally. At this point, the right eye was photographed while a diode-pumped solid state laser (emission 532 nm) was directed approximately perpendicularly at either the 'optical fold' or areas of the external ocular surface away from the fold which are composed of only the dermis and reflective argentea.

Subsequently, the two halves of the head were preserved for light and electron microscopy by immersion in 2.5% glutaraldehyde in 0.1 M phosphate buffer (pH, 7.4) for 2 days. They were then transferred to the same buffer and stored at 4 °C until and during transfer from the ship to the home laboratory, where they were postfixed in 2% osmium tetroxide. After thorough rinsing and dehydration, the two halves of the head were each embedded in Epon. Serial transverse sections (50 μm thick) were cut in a plane perpendicular to the long axis of the body with a steel knife, collected on plastic slides and photographed using a stereomicroscope. This method allowed us to isolate individual regions of interest and reembed them for cutting as semithin (1.5 μm) and ultrathin (50–100 nm) sections in the transverse, horizontal and sagittal planes. Thick and semithin sections were stained with

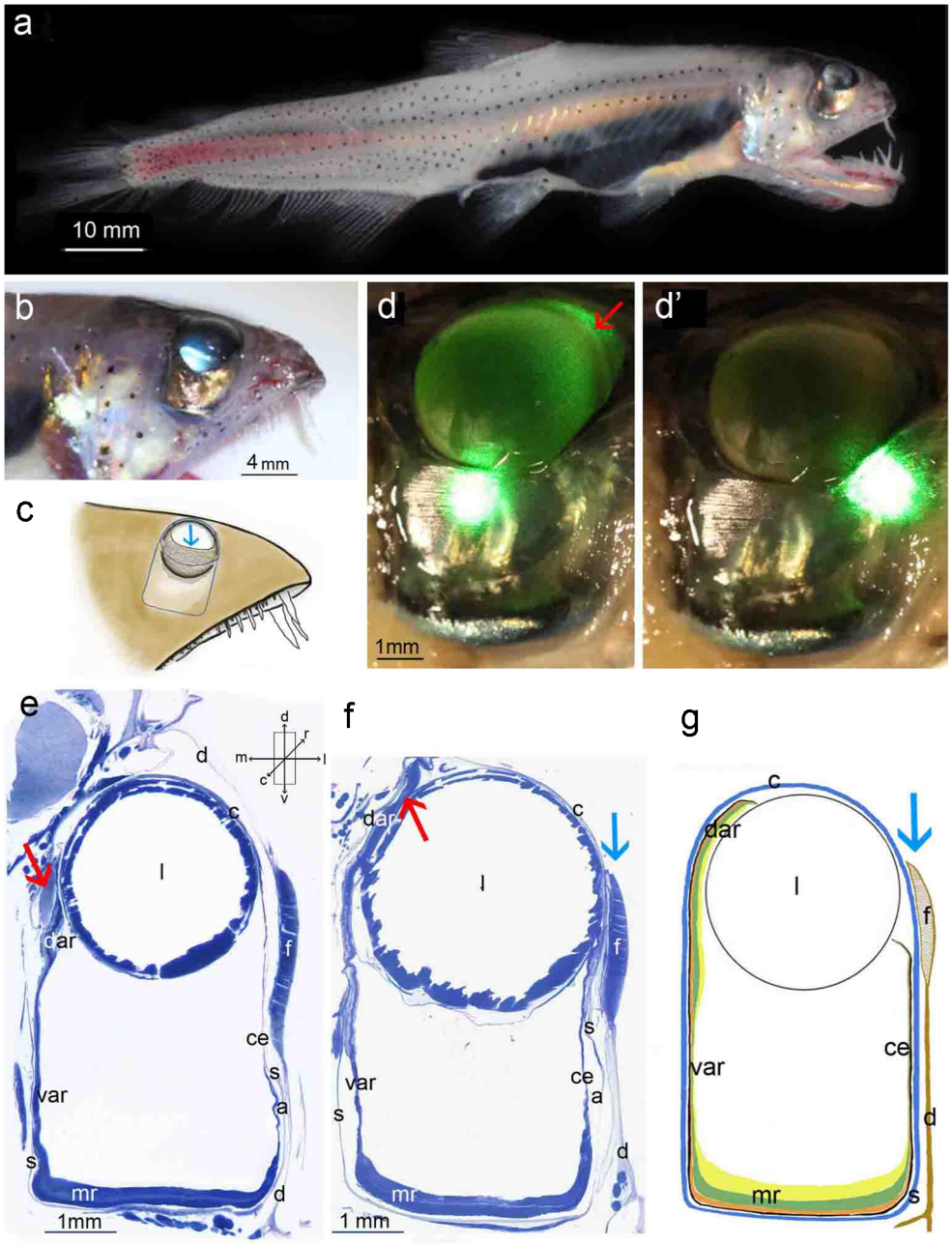

Fig. 1 **a**, **b** Fresh specimen of *Evermanella balbo* (photographs courtesy A. Flynn). **c** Drawing based on Fig. 1b illustrating the sclera/cornea (blue lines) and lens (thick black line and light grey area) covered by skin (brown) including the eyelid (dorsal free edge indicated by blue arrow) and the lamellar body of the 'optical fold' (indicated by the hatched area). **d**, **d**' Right eye of the fixed specimen photographed while a green diode-pumped solid state laser was directed approximately perpendicularly at the 'optical fold', resulting in illumination of the eye's interior and showing the transparency of the fold (**d**). Illumination of an area of the ocular surface composed only of the dermis and reflective argentea, did not result in the passage of light into the eye (**d**'); here and below, the red arrow indicates the accessory retina. **e** Thick (50 μm) transverse section of rostral region of the eye with the 'optical fold' in continuity with the dermis ventrally and dorsally. **f** Thick transverse section of the central region of the eye with the 'optical fold' overlying the cornea, originating from the dermis ventrally and tapering apically to a free edge, which is indicated by the blue arrow. **g** Schematic drawing based on Fig. 1f to assist in identifying the individual ocular layers. Starting externally, these layers are dermis (brown), sclera/cornea (blue), choroid (black), retinal pigment epithelium (orange), photoreceptors (green), inner retina (yellow). c, cornea; l, lens; d, dermis; f, 'optical fold'; mr, main retina; var, ventral accessory retina; dar, dorsal accessory retina; s, sclera; a, argentea; ce, ciliary epithelium. In order to facilitate orientation, the plane of sectioning relative to the body axis has been included in this, and all subsequent, figures (r, rostral; c, caudal; d, dorsal; v, ventral; m, medial; l, lateral)

methylene blue and Azur II (Richardson et al. 1960) and photographed with a Zeiss axioscope. Ultrathin sections were stained with lead citrate and electron micrographs obtained with a Leo EM912 and a digital camera. Adobe Photoshop

CS3 Extended was used for the preparation and labelling of the figures.

Studying the tubular eye of *Evermanella* and the 'optical fold', in particular, requires clearly defined planes of sectioning with respect to the body axes. These may differ from those used in mammals. We define as 'transverse' sections perpendicular to the long axis of the body; this would correspond to 'frontal' in mammals. 'Sagittal' and 'horizontal' are parallel to the long axis, with 'sagittal' in the dorso-ventral, and 'horizontal' in the medio-lateral plane.

Results

Gross ocular structure

Our specimen of *E. balbo* had upwardly directed tubular eyes approximately 5.0 mm wide and 7.4 mm in length when measured in the unfixed animal (Fig. 1b). In histological sections, all measurements were about 20% less due to tissue shrinkage during fixation (Steinberg et al. 1973) (Fig. 1e, f). Dorsally, the eyes are covered by an almost hemispherical cornea that reaches from its origin medially to the junction with the sclera ventral to the equator of the lens. The exact position of the ventral corneoscleral junction is not visible externally, as it is covered by a crescent-shaped eyelid-like structure (Fig. 1c–g) that is continuous with the transparent dermis ventrally, rostrally and caudally (Fig. 1e), but has a free dorsal edge centrally (Fig. 1c, f, g; blue arrow). In histological sections, even at low magnification (Fig. 1e, f), it is apparent that this fold contains tightly packed lamellar material. The optical nature of these lamellae is evident from the reflection ventral to the cornea in our fresh specimen (Fig. 1b) and that is why the 'eyelid' of *E. balbo* has previously been referred to as the 'optical fold' (Brauer 1908; Locket 1977). Illumination of the 'optical fold' with a laser shows that it permits incident light to enter the eye, even when fixed (Fig. 1d). Within the eye, this light is scattered by the artificially opaque lens illuminating much of the eye's interior, including the dorsal accessory retina (indicated by a red arrow in Fig. 1d). Light falling on areas of the eye's exterior not covered by the 'optical fold', however, does not enter the eye and is reflected by the argentea (Fig. 1d').

As in most tubular eyes, the ventral base of the *E. balbo* eye is covered by a well-developed 'main' retina. The lateral wall (medial to the choroidal argentea) is lined by a two-layered epithelium characteristic of the ciliary epithelium, while internally on the medial wall, the main retina tapers into a thinner accessory retina that increases in thickness dorsally as it approaches the crystalline lens (Fig. 1e–g).

Retinal fine structure

Based on morphological criteria, the *E. balbo* retina contains only rods. The cylindrical outer segments of all photoreceptors are completely ensheathed by a plasma membrane and contain free floating discs (Fig. 3e), and the synaptic terminals are small and have on average two synaptic ribbons (Fig. 3g). However, unlike rods in most other vertebrates, those in *E. balbo* show large cylindrical inner segments that may match the outer segments in size (Fig. 2a'–c').

The main retina of *E. balbo*, covering the base of the tubular eye, differs from the 'typical' deep-sea fish retina as its inner layers are well developed and similar in thickness to those of many visually oriented surface-living fish. As in the closely related *Scopelarchus michaelsarsi* (Collin et al. 1998), regional variations in the length and arrangement of rods are apparent within the main retina.

In the lateral third of the main retina, rod inner and outer segments (ris-ros) are about 70 μm long, and small bundles of them are incompletely separated by long, finger-like apical processes of the retinal pigment epithelium (rpe) (Fig. 2a, a'). This area of the main retina is also characterised by large ganglion cells with diameters up to 25 μm (Fig. 2a, arrows). In the centre of the main retina, the ris-ros combined length increases to 80–90 μm and rpe processes no longer separate the rods into bundles (Figs. 2b, b', and 3a, b). In this region, the packing, especially of the ris, appears denser than elsewhere, and the arrangement is regular and palisade-like. In the medial third of the main retina, ris-ros length increases further, exceeding 100 μm, but the packing is less dense than in the central retina (Fig. 2c, c'). All across the main retina, the rpe contains only moderate densities of melanosomes, which are located mainly in the perinuclear cytoplasm (Figs. 2a', c' and 3a). In addition, The rpe contains conspicuous stacks of parallel membranes ensheathing the photoreceptors. In the rpe

Fig. 2 Light micrographs of semithin 1-μm transverse sections through the central part of the eye illustrating the main and accessory retinae. Three areas of the main retina (**a**–**c**) and two areas of the accessory retina (**d**, **e**) are shown and their location indicated by corresponding red letters in the surrounding overviews (**f**, **g**) showing **f** the main retina and **g** parts of the accessory retina. **a**'–**c**' Higher magnifications of the outer retina near areas (**a**–**c**) of the main retina. **a**, **a**' are from the lateral main retina and show bundles of rods separated by largely unpigmented rpe apical processes (*): This area also contains conspicuously large ganglion cells (arrows). **b**, **b**' Densely packed rods in the central part of the main retina without grouping. **c**, **c**' in the medial part the main retina rods increase in length, are ungrouped and appear less dense than in **b**. **d** The ventral accessory retina contains short, ungrouped, rods. **e** Dorsally (roughly neighbouring the crystalline lens), the thickness of the accessory retina increases and groups of rods are separated by rpe processes filled with melanosomes (indicated by asterisks); arrows in **d** and **e** point to rod nuclei inside the outer limiting membrane (olm). gcl, ganglion cell layer; inl, inner nuclear layer; ipl, inner plexiform layer; n, nucleus; onl, outer nuclear layer; opl, outer plexiform layer; ris, rod inner segments; ros, rod outer segments; rpe, retinal pigment epithelium

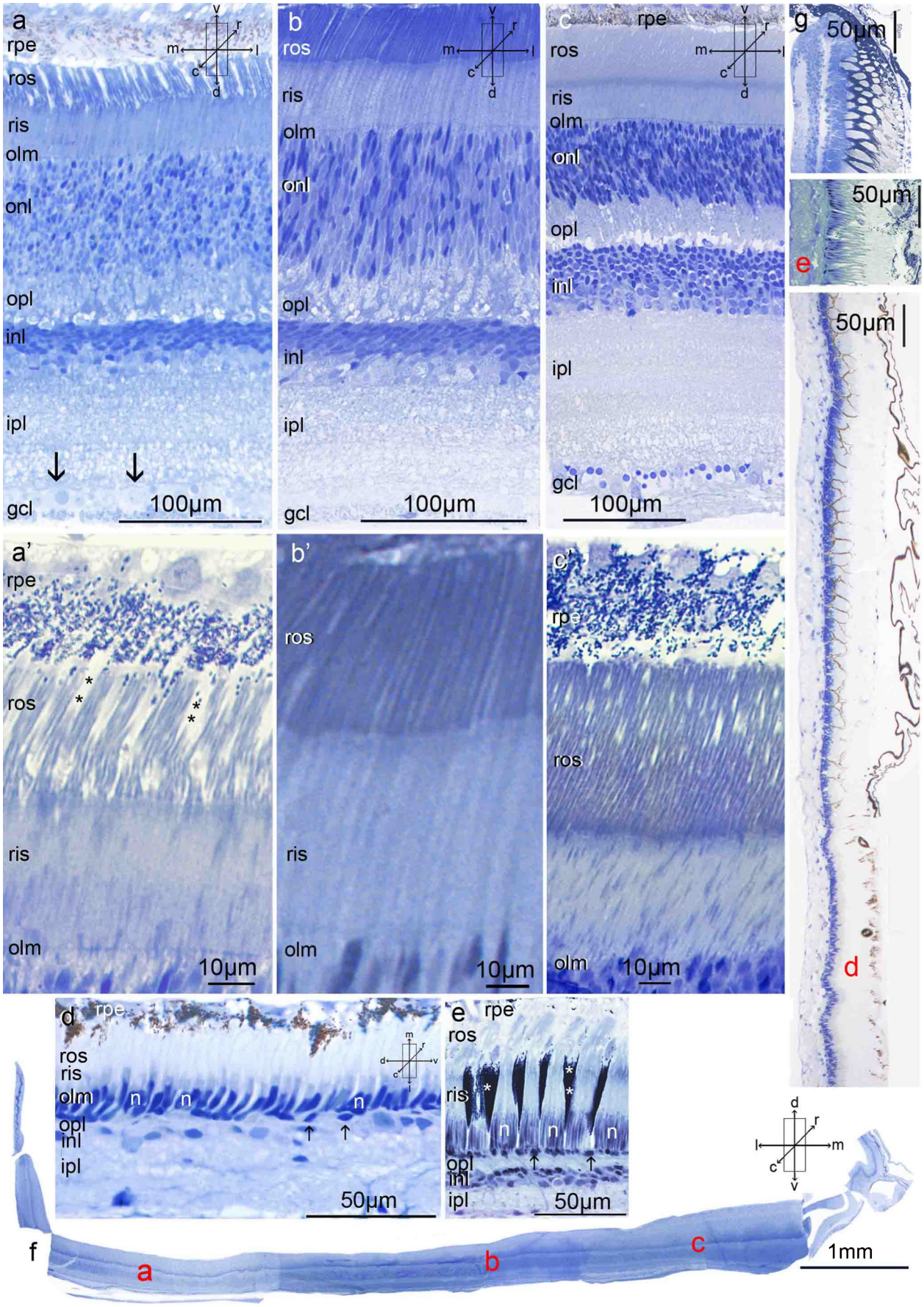
a
rpe
ros
ris
olm
onl
opl
inl
ipl
gcl
100μm
b
ros
ris
olm
onl
opl
inl
ipl
gcl
100μm
c
rpe
ros
ris
olm
onl
opl
inl
ipl
gcl
100μm
g
50μm
e
50μm
d
50μm
a'
rpe
ros
ris
olm
10μm
b'
ros
ris
olm
10μm
c'
rpe
ros
olm
10μm
d
rpe
ros
ris
olm
opl
inl
ipl
n
50μm
e
rpe
ros
ris
opl
inl
ipl
n
50μm
f
a
b
c
1mm

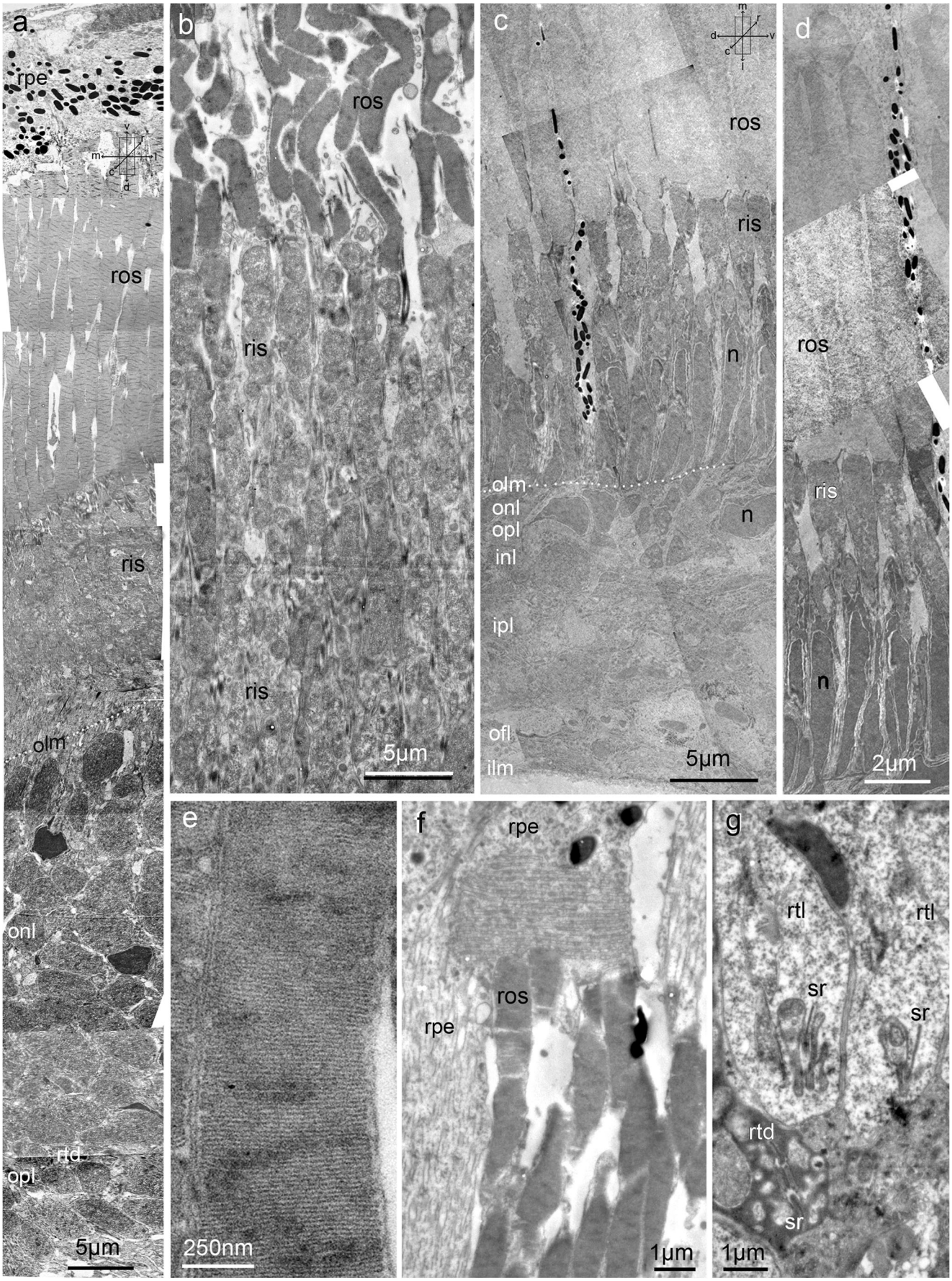
a.
rpe
ros
ris
olm
onl
rtd
opl
5μm
b
ros
ris
ris
5μm
c
ros
ris
n
olm
onl
opl
inl
n
ipl
ofl
ilm
5μm
d
ros
ris
n
2μm
e
250nm
f
rpe
ros
rpe
1μm
g
rtl
rtl
sr
sr
rtd
sr
1μm

◀ **Fig. 3** Electron micrographs of the retina of *Evermanella balbo* (**a**, **b**) areas of the central main retina containing ungrouped receptors. **c**, **d** Regions of the accessory retina with grouped rods some of whose nuclei lie external to the outer limiting membrane. **e** Rod outer segment from the accessory retina showing isolated discs floating within a common outer segment membrane. **f** Within the rpe of the lateral main retina, stacks of membranes lie parallel to the length of the outer segment and at its tips are stacked perpendicularly. **g** Small photoreceptor synaptic terminals contain, on average, about two synaptic ribbons; in the accessory retina, the rod terminals come in two varieties, either with light or with dark cytoplasm. ilm, inner limiting membrane; inl, inner nuclear layer; ipl, inner plexiform layer; n, nucleus; ofm, optic fibre layer; olm, outer limiting membrane (indicated by dotted line); onl, outer nuclear layer; opl, outer plexiform layer; ris, rod inner segments; ros, rod outer segments; rpe, retinal pigment epithelium; rtd, rod terminal dark; rtl, rod terminal light; sr, synaptic ribbon

processes, these run parallel to the ros, while abutting their tips, they lie perpendicularly (Fig. 3f). The empty spaces between these membranes most likely contained guanine crystals, forming a reflective tapetum within the rpe, that were dissolved during histological processing.

The transition from the ca. 400-μm thick medial main retina (Fig. 2a) to the accessory retina is marked by a sharp decrease in thickness to barely 100 μm (Figs. 1e–g, and 2g). Although this thinning occurs in all retinal layers, the inner retina is most strongly affected. An unusual feature, observed throughout the accessory retina, is that many, but not all, of the rod nuclei lie external to the outer limiting membrane (olm) (Figs. 2d, e and 3c, d). The different localisation of some nuclei inside and others outside the limiting membrane, as well as the observation that some rod spherules have light and others dark cytoplasm (Fig. 3g), might indicate the presence of two types of rod in the *E. balbo* accessory retina.

In the ventral half of the accessory retina, the rods are about 30 μm long, show no regular arrangement and are not grouped into bundles (Fig. 2d). rpe cells in this region resemble those in the main retina, as their melanosomes are mostly located in the perinuclear cytoplasm rather than in the apical processes. Two significant morphological changes occur in the dorsal half of the accessory retina: Firstly, dorsally located rods are arranged into distinct bundles, separated by sheet-like, melanosome-filled, apical rpe processes (Figs. 2e and 3c, d). Secondly, the overall thickness of the retina increases abruptly dorsally, reaching 150–200 μm as it approaches the crystalline lens (Figs. 1e, f and 2 g). This affects all layers, but ris-ros length in particular. Compared to the rod groups in the lateral main retina, which comprise between 20 and 30 ris-ros bundles, in the dorsal accessory retina, the bundles are much larger and contain up to 200 photoreceptors. At the extreme dorsal edge of the accessory retina (Fig. 2g top), the packing of rods within a bundle is densest and the bundle diameter smallest (about 25–30 μm). Unlike in the main and ventral accessory retinas, the perinuclear cytoplasm of rpe cells in the dorsal accessory retina is almost devoid of melanosomes (Figs. 2e, and 3c) and probably forms a tapetum capable of reflecting incident light. Instead, the melanosomes are concentrated in the apical processes of the rpe cells, resulting in the optical isolation of individual bundles of photoreceptors in the dorsal accessory retina.

Structure of the 'optical fold'

As noted above, the ventral cornea of *E. balbo* is covered by a crescent-shaped structure superficially resembling the lower eyelid of many vertebrates (Figs. 1b–g). This is continuous with the transparent dermis ventrally, rostrally and caudally (Fig. 1e), but has a free dorsal edge centrally (Fig. 1c, f, g). In Fig. 4a, the dorsal edge of this 'eyelid' has broken off and appears to be fused with the cornea. However, it is not. More ventrally, there is an obvious cleft separating the 'eyelid' and the cornea, which terminates at the conjunctival fornix where the stratified corneal epithelium is reflected dorsally to become a simple squamous epithelium on the medial surface of the 'eyelid' (Fig. 4a, arrow). The lateral surface of the 'eyelid' is covered by an epithelium characteristic of the epidermis (Figs. 4c and 5c) that increases in thickness ventrally; the transition between the two epithelia on the different 'eyelid' surfaces occurs at the dorsal tip of the fold. Both epithelia are separated by a prominent basal membrane from the underlying propria region of connective tissue (Figs. 4b, c and 5c) which consists of fibrocytes and matrix that show no obvious regular arrangement.

The substantial inner core of the 'eyelid' is formed by lamellar material running approximately perpendicular to its medial and lateral surfaces. Due to the presumed optical function of these lamellae, the 'eyelid' in *Evermanella* has been termed an 'optical fold' (Locket 1977). However, the area containing the lamellae extends beyond the bounds of the 'eyelid'. The approximate extent of the lamellae in our fresh specimen is represented externally by the reflective area around the ventral cornea in Fig. 1b, which extends 4.1 mm in the rostro-caudal direction and 2.2 mm dorsoventrally. As the dorsal free rim of the 'eyelid' spans only about 3 mm (Fig. 1b–d), the lamellae extend beyond its rostral and caudal edges. The distance from the dorsal edge of the 'eyelid' to the conjunctival fornix in histological sections is only about 1.1 mm, so that about half of the lamellar body lies ventral to the 'eyelid' fold (Figs. 1e, f and 4a). Thus, the term 'optical fold' may not be wholly appropriate for this structure, as much of the lamellar body, which we presume has optical properties, extends beyond the superficially visible 'fold' of the 'eyelid'. The term 'optical fold' is nonetheless retained for historical consistency, and refers to all of the lamellar body, even that not within the 'eyelid'.

The shape of the 'optical fold' in transverse section is slightly convex on its medial surface, loosely following the external contour of the crystalline lens, and tapering both

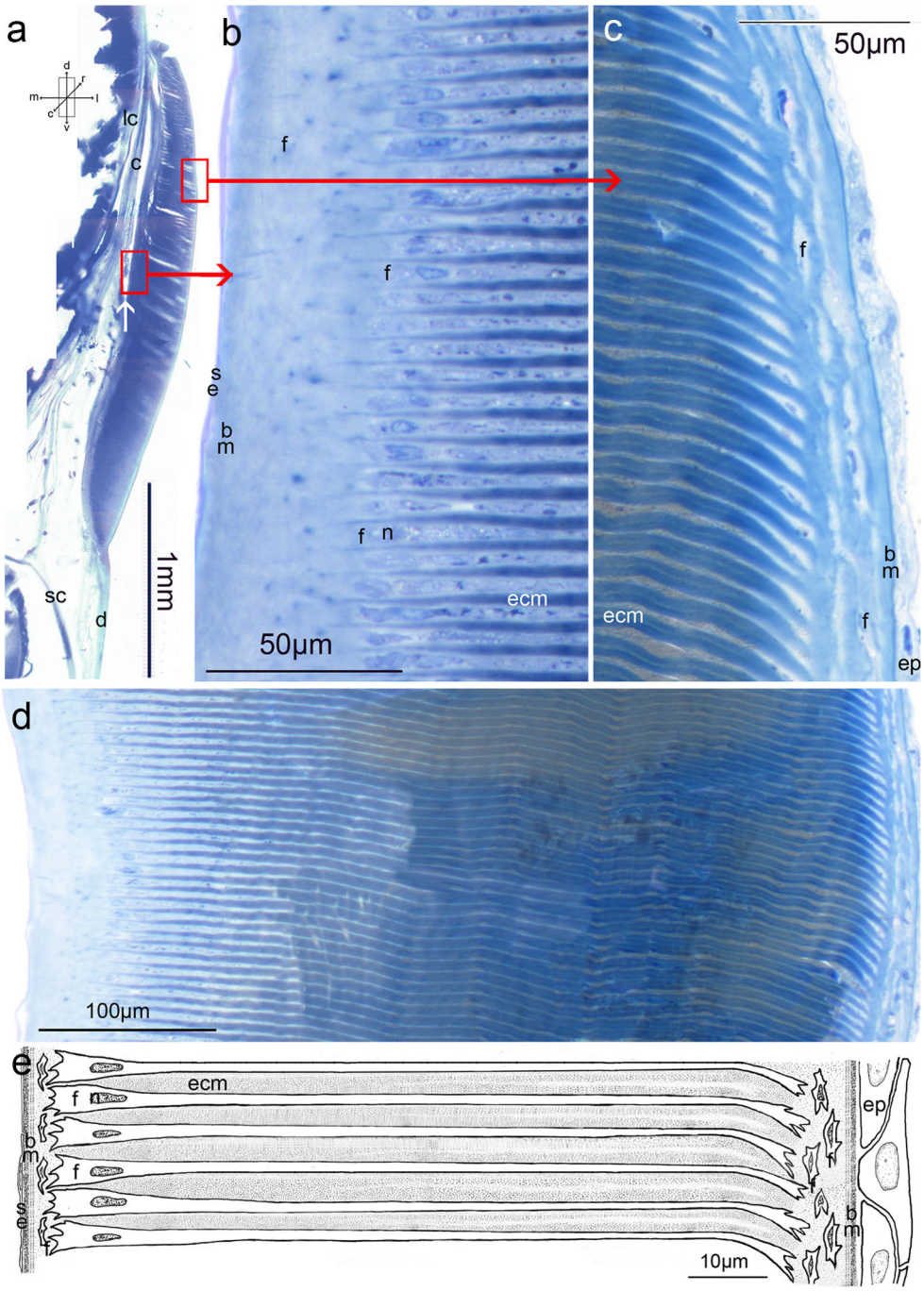

Fig. 4 Light micrographs of the 'optical fold' (**a**) thick (50 μm) section of the 'optical fold' and adjacent structures, boxes and arrows point at higher magnification micrographs of the semithin sections shown in **b** and **c**. The white arrow indicates the conjunctival fornix where the corneal epithelium is reflected onto the simple epithelium on the inside of the eyelid. The lens stroma is absent as it fragments during sectioning. The lamellae are not oriented perfectly horizontally, but are tilted by about 20° from the horizontal. In the subsequent figures, they are, however, shown so that they appear to be horizontal. **b** Semithin section of the medial surface of the 'optical fold', orientation as in **a**. **c** Semithin section of the lateral surface of the 'optical fold', orientation as in **a**. **d** Semithin section of the entire width of the 'optical fold'. **e** Schematic representation of the histological organisation of the 'optical fold'. bm, basal membrane; c, cornea; d, dermis; ecm, extracellular matrix and material (collagen fibrils); ep, epidermis; f, fibrocyte; lc, lens capsule; n, nucleus; sc, sclera; se, simple epithelium

dorsally and ventrally (Figs. 1e, f and 4a); its maximal thickness in histological sections is 0.45 mm.

Within the 'eyelid', about 20–30 μm lateral to its medial border, the fibrocytes in the connective tissue underlying the basal lamina of the simple epithelium take on a palisade-like orientation roughly perpendicular to the surface, forming lightly-staining lamellae. The nuclei of these cells are vertically stacked at about equal distances from the medial basal membrane (Figs. 4b and 5a). Ventral to the conjunctival fornix, the inner simple epithelium of the 'eyelid' along with the basal membrane is absent, and the lamellae are embedded medially in the episcleral connective tissue, equivalent to the reticular layer of the dermis. Laterally, these palely-staining fibroblastic cells extend long cytoplasmic processes that seem to run uninterrupted towards the lateral edge of the fold (Fig. 4d, e) or infrapalpebral skin, where they terminate among the propria layer of the dermis. These processes are arranged in regular, parallel layers with a width of about 5 μm medially, tapering to about 2 μm laterally.

They contain sparse mitochondria and membrane systems of the endoplasmic reticulum.

The darker extracellular material between the pale fibroblastic lamellae is presumably made up of glycosaminoglycans and proteoglycans in which highly organised and regular arrays of electron-dense collagen fibrils are embedded (Figs. 5b and 6). The characteristic banding of fibrillar collagen is shown in the inset of Fig. 6d. Nearest to the plasmalemma of each of the adjacent fibroblastic cellular lamellae, there is a region 400–500 nm wide made up of thin fibrils each with a diameter of about 25 nm and a spacing of about 20 nm. Between these two peripheral layers, the remaining volume is filled with thicker fibrils ca. 50 nm in diameter that vary in spacing from 40 to 100 nm (Fig. 6a). For a more detailed analysis of the 3D organisation of the collagen fibrils, we examined sections cut not only in the transverse plane (as shown in Figs. 1e–g or 4) but also in horizontal and latero-sagittal planes (i.e. parallel to the surface of the fold). Figure 6c shows the arrangement of the thin fibrils lying in the horizontal plane organised in alternating sheets. In each sheet, fibrils are parallel, but with their orientation changing by 90° between each sheet. By contrast, all the thick fibrils are oriented parallel to the lateral surface of the fold (Fig. 6b, d) so that they are seen in cross section in the transverse plane (Fig. 6a). The schematic drawing of the central inset (Fig. 6e) illustrates the arrangement of thin and thick fibrils in the extracellular component of the lamellae in the 'optical fold'.

The 'optical fold' is thus a lamellar body of regular alternating light (cytoplasmic) and dark (extracellular) stained bands seen in both LM and TEM sections. Medially, the lamellae are straight, while laterally, they are slightly curved in the ventral direction. Overall, the lamellae are tilted approximately 20° from the horizontal (their medial aspect lying above the horizontal) (Figs. 1e, f and 4a), which will likely impact on their optical properties. As noted above, the relative width of the light and dark bands changes from medial to lateral resulting in lightly staining cytoplasmic bands of about 2–2.5 μm thickness, and extracellular dark bands 4.5–5 μm thick when measured at the centre of the 'optical fold' (Figs. 4d, and 5b). Measuring the number of light/dark lamellar pairs over a dorso-ventral distance of 4 mm in several sections of the 'optical fold' results in an average width of 6.7 μm for each pair (5.5 μm minimum and 7.1 μm maximum).

Discussion

Structure of the retina

Brauer (1908) examined the retinae of two species of *Evermanella*, *E. balbo* and *E. indica*, of which the latter species was also studied by Munk (1966). The main retina covering the base of the *E. balbo* tubular eye is well-developed, showing all the layers characteristic of a vertebrate retina,

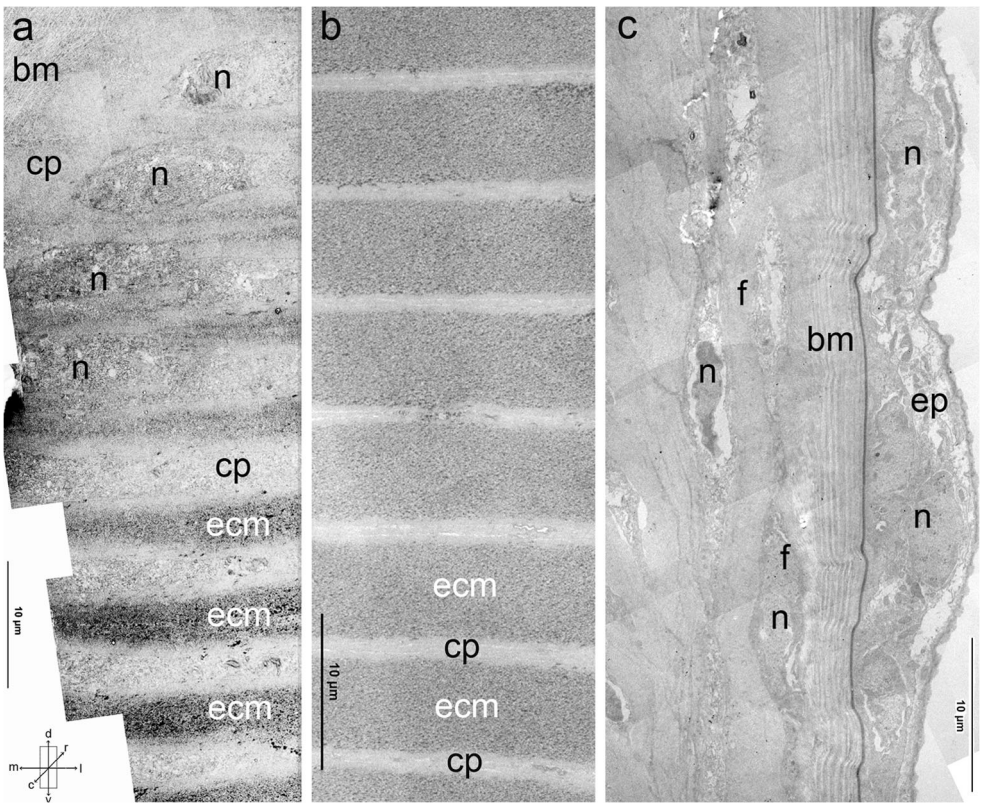

Fig. 5 Low power electron micrographs of the 'optical fold' **a** medial surface. The light stripes represent cytoplasm (cp) and the dark stripes extracellular matrix and collagen fibrils (ecm). **b** Central region. **c** The lateral surface. bm, basal membrane; ep, epidermal epithelial cells; f, fibrocyte; n, nucleus

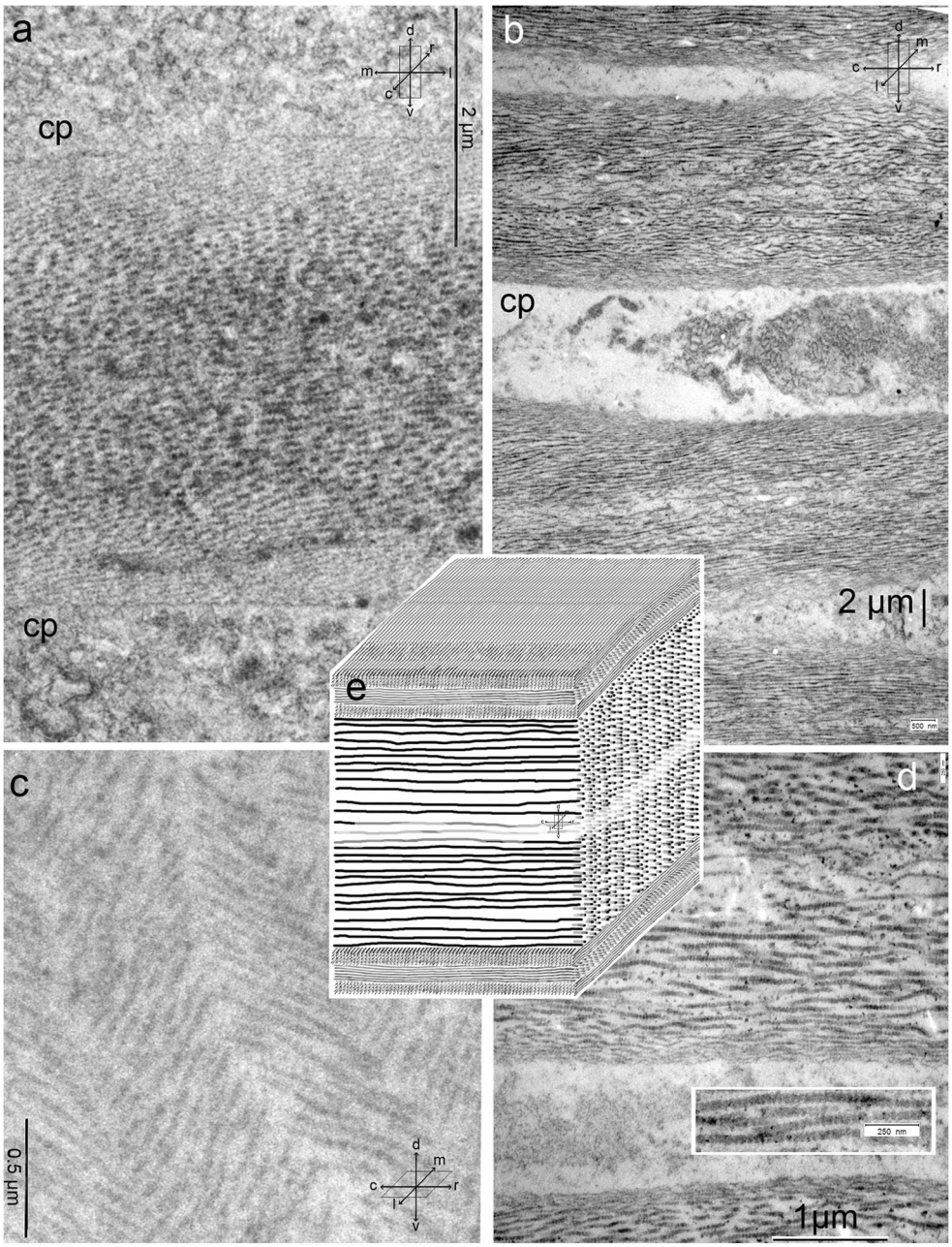

Fig. 6 Electron micrographs of the 'optical fold' matrix regions to illustrate the 3D organisation of the collagen fibrils (central inset). **a** Transverse plane shows thin fibrils (25 nm diameter; spacing about 20 nm) adjacent to the cytoplasmic regions and thicker fibrils (50 nm; spacing 40–100 nm) in the middle of the extracellular matrix area, mostly seen in cross section. **b**, **d** Sections in a latero-sagittal plane. The majority of the thick fibrils (seen in transverse section in Fig. 6a) run longitudinally, parallel to the surface of the fold. **c** Horizontal plane at the level of the thin fibrils, cutting through adjacent layers of thin fibrils. These are arranged in narrow sublaminae with parallel fibrils that are offset by 90° within each sublamina. High magnification inset in **d** shows banding of fibrils characteristic of fibrillar collagen types. cp, cytoplasmic regions of fibroblastic lamellae. **e** Schematic illustration of the arrangement of thin and thick collagen fibres in the extracellular component of the lamellae in the 'optical fold'. In this schematic, the number of thick fibrils is not representative of the true number (see Fig. 6a) and only three layers of thin fibrils are shown, whereas this number could be more

while the accessory retina, as in other tube-eyed species, is much reduced. Both the main and accessory retinae are not homogenous, and exhibit areas of morphological specialisation.

Photoreceptor identity

The retinae of most vertebrates contain two types of differentially sensitive photoreceptors: rods, active at low light levels and cones, which function in brighter illumination. These two photoreceptor classes, coupled to the biochemical and physiological mechanisms of light and dark adaptation (Lamb and Pugh 2004; Perlman and Normann 1998), allow most vertebrates to retain useful vision over a large range of light levels (up to 10 log units), which is beyond the dynamic range of any one photoreceptor type.

As the two sources of illumination in the deep sea, downwelling sunlight and bioluminescence, are both of low intensity, most deep-sea fish have retinae containing only rods (Locket 1977; Wagner et al. 1998). The retina of *E. balbo* also appears, on morphological grounds, to contain only rods. The only photoreceptor terminals observed were small, consisting of a single invagination with an average of two synaptic ribbons (Fig. 3g), which is typical of teleost rods. Furthermore, the discs within the outer segments were 'free floating' and unattached to the

plasma membrane (Fig. 3e), another defining characteristic of rods.

However, the distinction between rods and cones is not always as clear as it at first sight might seem, as some photoreceptors exhibit morphological, electrophysiological and molecular characteristics of both rods and cones (Underwood 1968; Dickson and Graves 1979; Dowling and Ripps 1990; Munk and Rasmussen 1993; Röll 2000; Ma et al. 2001; de Busserolles et al. 2017; Simões et al. 2016; Schott et al. 2016). The existence of such hybrid photoreceptors in some reptiles led Walls (1934, 1942) to propose the transmutation theory, in which one photoreceptor class evolves into another via a series of intermediates as animals adapt to different photic environments.

Interestingly, unlike rods in most other vertebrates, those in *E. balbo* show large cylindrical inner segments, a characteristic usually associated with cones. These enlarged rod inner segments were also seen by Munk (1966) in *E. indica*, which, along with some other cone-like features, prompted him to suggest that although the photoreceptors in this species were rods, in line with Walls's theory, they were phylogenetically derived from cones.

While it appears unlikely that the retina of *E. balbo* contains any cones, it is possible that this species has two populations of morphologically distinct rods, at least in the accessory retina. While some rod nuclei, like those of most vertebrates, lie inside the olm, in the accessory retina of *E. balbo*, most rod nuclei are positioned external to the olm (Munk 1966; Figs. 2d, e and 3c, d). The scleral positioning of nuclei is a cone-like feature and has also been observed in the closely related *Scopelarchus gűntheri* (Locket 1971). Another indication of two classes of rods comes from the observation that rod spherules can either have a dark or a light cytoplasm (Fig. 3g). While variation in electron density is often attributed to fixation artefacts, this may not be true for the electron-light and -dark rod spherules observed here, because this difference is present only in the accessory retina and absent in the main retina, where only the dark variety is observed (Fig. 3a). This correlates with the two positions of rod nuclei in the accessory, but not the main, retina.

Although such morphological evidence for two types of rod in *E. balbo* is far from conclusive, it is supported by the observation that the retinal transcriptome of *E. indica* expresses both *rh1* and *rh2* visual pigment genes (de Busserolles and Cortesi, pers. com). Although *rh2* pigments are usually found in cones, de Busserolles et al. (2017) observe two morphological types of rods in a genus of mesopelagic teleost, *Maurolicus sp.*, one of which contains *rh*1-based pigments and the other *rh2* pigments. In fact, there are several other examples of cone visual pigment genes being expressed in morphological rods and vice versa (Kojima et al. 1992; McDevitt et al. 1993; Kawamura and Yokoyama 1997; Yokoyama and Blow 2001; Ma et al. 2001; Hart et al. 2012; Simões et al. 2016; Schott et al. 2016). The visual pigments of *E.balbo* have not been measured by microspectrophotometry (MSP), which could identify where different visual pigments (if present) are located in the retina. However, MSP measurements in a related Alepisauroidid, *Scopelarchus analis*, showed that up to three visual pigments, with different λ_{max} values, were expressed in rod-like cells in both accessory and main retinae (Partridge et al. 1992). It is therefore plausible that *E. balbo* has both more than one type of photoreceptor and more than a single visual pigment.

Regional variation

Main retina As in *Scopelarchus spp.* (Locket 1971; Collin et al. 1998), the main retina of *E. balbo* contains both areas of individual rods and regions where 20–30 rods are grouped into bundles incompletely separated by largely unpigmented rpe apical processes. However, the bundles may nonetheless be optically isolated from one another as the rpe processes most likely contain reflective crystals that ensheath each group of rods, although these are lost during embedding and appear as holes in histological sections (Fig. 3f).

In teleost fish, a well-focussed image is produced when the eye obeys Matthiesen's ratio, where the distance from the centre of the lens to the retina divided by the lens radius is around 2.55 (Fernald 1990). Since the main retina of *E. balbo* conforms to this ratio (2.58; Fig. 1e–g), the image projected on to it has the potential for high spatial resolution. The highest resolution within the main retina is most likely provided by the central (Fig. 2b, b') and medial (Fig. 2c, c') regions where individual rods are tightly packed. Resolution will of course ultimately depend on the degree of post-receptoral summation of the photoreceptor output. In most deep-sea fish, the inner retinal layers are not well-developed as there is a high degree of convergence of numerous rod photoreceptors onto small numbers of bipolar and ganglion cells to ensure maximal sensitivity. Unusually for the retina of a deep-sea fish, the inner retina of *E. balbo* is extensive, suggesting a reasonable degree of spatial resolution is possible.

In contrast, the lateral part of the main retina is unlikely to provide high spatial resolution in *E. balbo* as its photoreceptor inner and outer segments are grouped into bundles (Fig. 2a, a'). Such grouped photoreceptors, often surrounded by reflective crystals (Fig. 3f) and joined by electrical synapses (Collin et al. 1998 for review), are only found in teleost fish. Since grouped retinae are mainly associated with species inhabiting dimly lit environments, they are considered an adaptation for enhanced sensitivity. They are perhaps most well known in mormyrid electric fish, but are also observed in other freshwater and deep-sea species (Francke et al. 2014 for review). Each bundle of photoreceptors is thought to act as a functional unit,

forming a macroreceptor (Locket 1971) where the outputs of all the photoreceptors within a group are combined, resulting in a detector with a large receptive field (Warrant and Locket 2004). This suggestion receives support from the observation that the dendritic field size of some bipolar cells in the elephantnose fish (*Gnathonemus petersii*) matches the diameter of the photoreceptor bundle they serve (Wagner 2007). Such an arrangement optimises sensitivity at the expense of spatial resolving power.

The lateral main retina of *E. balbo* with grouped photoreceptors also contains a population of ganglion cells with unusually large cell bodies (Fig. 2a, arrows). Similar alpha-like ganglion cells have been observed in the caudal retina of *Scopelarchus michaelsarsi* (area gigantocellularis, Collin et al. 1998) as well as throughout the retina of other vertebrates, and it has been suggested that they are involved in motion detection. In weakly electric mormyrid fish, electrophysiological and anatomical data also suggest that grouped retina may improve motion detection, especially to low spatial frequencies and at reduced contrast (Francke et al. 2014).

Thus, the medial and central ungrouped regions of the main retina of *E. balbo* most likely subserve higher spatial acuity vision, while the grouped receptors of the lateral retina are specialised for sensitivity and motion detection.

Accessory retina The accessory retina, covering the medial, as well as part of the rostral and caudal, walls of the tubular eye of *E. balbo*, is, as in other tube-eyed teleosts, much reduced throughout its extent compared to the main retina (Figs. 1e, f and 2g). It is particularly poorly developed ventrally where short individual rods make up a retina of no more than 100 μm thickness. However, the accessory retina increases in thickness and complexity dorsally, where it is adjacent to the lens. Here the photoreceptors are grouped into bundles which are separated by heavily pigmented apical rpe processes (Figs. 2e, g and 3c, d), while the perikarya of the rpe cells are almost devoid of pigment (Figs. 2e and 3c; Brauer 1908; Munk 1966). Although the thin accessory retina of tubular eyes is often slightly more developed dorsally than it is ventrally (Locket 1977), the degree of increased complexity of this region described here for *E. balbo* is, as far as we are aware, unique to this species.

Grouped photoreceptors were also described in *Scopelarchus spp.*, although in this genus they were distributed throughout the accessory retina (Locket 1971; Collin et al. 1998). As noted above, the grouping of a large number of rods (up to 200) into optically isolated bundles in the dorsal accessory retina of *E. balbo* will result in enhanced sensitivity, and probably motion detection, but at the expense of low spatial resolving power. This is of some significance as the dorsal accessory retina is where light that has passed through the 'optical fold' will almost certainly fall (see below).

The 'optical fold'

Structure

Brauer (1908) described a transparent fold of the skin, sometimes referred to as an adipose eyelid (despite the fact it contains no fatty tissue), which covers most of the ventral and lateral cornea of *Evermanella spp.,* leaving only the dorsal part uncovered. He noted it was largely composed of alternating lamellae of nucleated (cellular) and acellular material running perpendicular to the ocular surface, flanked medially and laterally by small regions of looser connective tissue. This was confirmed in a review by Locket (1977) for another Evermanellid (*Coccorrela atrata*), who additionally described a simple epithelium covering the medial surface and a basement membrane covering the fold medially and laterally. Due to the presumed optical function of this lamellated structure (see below), it has been referred to as an 'optical fold' (Locket 1977). However, as outlined above, this term is perhaps not entirely appropriate as the lamellae that make up the bulk of this structure extend beyond the borders of the 'eyelid' in rostral, caudal and ventral directions. Much of it thus lies outside the confines of the 'fold' making up the 'eyelid'.

Our observations support most of these basic findings of Locket (1977), but they differ in some details. For example, while Locket (1977) commented on the absence of an epithelium for the lateral surface of the fold, we observe epithelia on both surfaces (Figs. 4 and 5c). Similarly, Locket (1977) observed that the individual cells making up the cellular lamellae did not extend the width of the structure, whereas we find that they do, as evidenced by a single layer of nuclei medially (Figs. 4b and 5a). Interestingly, Locket (1977, Fig. 28) placed these nuclei laterally; we assume his figure was inadvertently inverted.

More importantly, our current observations significantly extend those of Brauer (1908) and Locket (1977) in some important respects. For example, we find the lamellae making up the 'optical fold' extend beyond the confines of the 'eyelid' caudally, rostrally and ventrally. Furthermore, we determine the thickness of the cellular and acellular lamellae mostly running perpendicular to the lateral ocular surface and note that they taper and turn ventrally near the lateral margin of the fold. We show the cellular lamellae are made of fibroblastic cells containing few organelles, while the extracellular lamellae are each made of two layers of thin collagen fibrils sandwiching a central layer of thicker collagen fibrils. For the first time, we also describe the three-dimensional organisation of the collagen fibrils. While all the thicker collagen fibrils run in a plane tilted by 20° from the horizontal with respect to the fold's surface, the flanking thinner layers are composed of several

sheets in which collagen runs at 90° to those in adjacent layers (Fig.6). When seen in a section slightly angled to the plane of these fibrils, they form a herring bone pattern (Fig. 6c).

Function

The primary purpose of this paper is to provide an accurate description of the anatomy and histology of the unusual eye of *Evermanella balbo*, and particularly the 'optical fold' observed on its lateral aspect. Nevertheless, curiosity about the function of the 'optical fold' provided a fundamental incentive for this study, and we therefore hope that the detailed anatomical and histological description presented here will provide the information needed for future theoretical interpretations of optics of this unusual ocular structure, ideally supported by optical measurements on fresh samples.

Nevertheless, it is possible to suggest what the 'optical fold' might achieve. Firstly, observations of the Evermanelid 'optical fold' show that it is transparent to incident light, whereas adjacent ocular tissue on the surface of the eye is not (Fig. 1d, d'). Secondly, those deep-sea fish that have retinal diverticula (see introduction) all extend their fields of view to image light originating from the ventro-lateral visual field where bioluminescent emissions will be seen against dim upwelling light or (at night) profound darkness. The detection of such an inherently high contrast visual signal is an easier sensory task than that of, for example, detecting bioluminescence that is seen against any remnant downwelling sunlight. It is therefore reasonable to infer that the Evermanelid 'optical fold' is likely to also extend the animal's visual field in the ventro-lateral direction.

What is not known, however, is whether or how the Evermanellid 'optical fold' redirects incident light, or to what extent it enhances the focus of light on the accessory retina. Locket (2000) shows that the lens pad of *Benthalbella* spreads incident light from below, via the ocular lens, into a poorly focused vertical streak on the accessory retina and argues that this will enable the fish to determine the direction of a bioluminescent event in the horizontal azimuth, but not in the vertical one. It is possibly that the slightly tilted laminations within the 'optical fold' of *Evermanella* produce a similar effect (despite the very different scale of the laminations in this genus; see below). Locket (1977) also showed that the 'optical fold' of *Coccorella* (another Evermanellid) has an ability to divert a latero-ventrally incident beam of light, presumably as a result of the alternating layers of cellular and collagenous lamellae described here having different refractive indices (Johnson 2012) and therefore being able to deviate the path of incident illumination.

Given its proximity to the lens (Fig. 1e–g), most light that traverses the 'optical fold' will enter the ocular lens and most likely be refracted by it to reach the dorsomedial accessory retina. However, this part of the retina is far too close to the lens to allow any degree of image formation by the lens alone. Ideally, the 'optical fold' would provide a fully functional secondary lens that, acting in synergy with the main ocular lens, would have sufficient diopteric power to produce a focused image of a bioluminescent source, or any other object. This would maximize the contrast of the image on the accessory retina, considerably increasing the ease with which the object could be detected. Such an adaptation is therefore likely to be under high selective pressure, but to do so the 'optical fold' would need to have a diopteric power similar to that of the main ocular lens. The absence of high refractive index elements, or structures indicating the presence of well-organized refractive index gradients typical of fish ocular lenses (Fernald 1990), suggests this is unlikely, unless the 'optical fold' employs a novel mechanism for light focusing that only further study and appropriate optical modelling can reveal.

It is important to note, however, that even if a focussed image was formed on the dorsal accessory retina, the spatial resolution provided will be very limited since the photoreceptors here occur in bundles acting as macroreceptors. The spatial resolution of this part of the retina would be defined by the visual angle subtended by a single bundle, resulting in large visual fields for each bundle. Therefore, the 'optical fold' of the Evermanellidae is most likely a light collector, rather than a high resolution imaging device. While a focussed image would increase both spatial resolution and sensitivity, unfocussed illumination is preferable to no light at all, and an optical adaptation providing even unfocussed light will allow the detection of the movement of a high contrast object or a bioluminescent flash ventro-lateral to the animal, which would be missed by a conventional tubular eye.

Comparison of the 'optical fold' of Evermanellidae to the lens pad of Scopelarchidae

Although the 'optical fold' described here is unique to the Evermanellidae, the 'lens pads' of the closely related Scopelarchidae are, superficially at least, very similar in both structure and presumably function (Brauer 1902, 1908; Munk 1966; Locket 1977, 2000). Like the 'optical fold', lens pads are lamellated structures positioned ventrolaterally immediately adjacent to the eye. However, unlike the 'optical fold', which is located external to the eye, partly within an eyelid-like structure, the lamellae making up the bulk of lens pads are thought to originate from, and be a continuation of, the cornea, and are separated from the eye's interior by little more than a simple endothelium (Locket 1977, 2000). The lamellae of the 'optical fold's of Evermanellidae are thus much further removed from the interior of the eye than in Scopelarchidae lens pads. Furthermore, the lamellae are of very different dimensions in the two structures. While in lens pads, a pair of light and dark lamellae are around 339 nm thick (Locket 2000), in

the 'optical fold' of *E. balbo* studied here they are around 20 times this width (6.7 μm). The size of the Scopelarchid lamellae, therefore, corresponds more to the fine-structural organisation of the collagen fibrils in the Evermanella stroma lamellae. The highly regular arrangement of equidistant, parallel fibrils of equal diameter, arranged in layers of alternating orientation (Fig. 6e) is reminiscent of the structure of human corneal stroma (Meek and Knupp 2015) and may similarly be expected to result in the optical transparency shown here (Fig. 1d).

As noted above, ophthalmoscopy shows that light entering the lens pad of a Scopelarchid (*Benthalbella infans*) from below, which in the absence of the pad would not impinge on the retina, is deviated by the pad into the lens and strikes the dorsal accessory retina (Locket 2000). It is presumed that the 'optical fold' of Evermanellids described here similarly acts to funnel ventrolateral light into the lens to illuminate the dorsal accessory retina (see above). However, while 'optical fold's probably function by refracting light, the smaller dimensions of the lamellae within Scopelarchid lens pads suggest they may transmit ventrolateral illumination by light guiding (Locket 1977). However, at this point, this is purely speculative.

Acknowledgements We are grateful to the master and crew of the FS Sonne and the chief scientist during cruise 234-1, Reinhard Werner. The technical expertise of Ulrich Mattheus is, as always, much appreciated. We are indebted to Adrian Flynn, who was responsible for the identification and photography of the specimen. Fanny de Busserolles and Fabio Cortesi kindly provided unpublished data on *Evermanella* photopigment opsins.

Compliance with ethical standards

Conflict of interest The authors declare that they have no conflict of interest.

HJW was funded by BMBF 03G0233B and 03G0258B.

Ethical approval All applicable international, national, and/or institutional guidelines for the care and use of animals were followed. The single animal used for this study was already dead due to temperature and pressure gradients when the net came on board, and was donated by the University of Queensland capture team for further study.

References

Brauer A (1902) Über den Bau der Augen einiger Tiefseefische. Verhandlungen der Deutschen zoologischen Gesellschaft (Leipzig) 12:42–57

Brauer A (1908) Die Tiefseefische. 2. Anatomischer Teil. Wissenschaftliche Ergebnisse der Deutschen Tiefsee-Expedition auf dem Dampfer 'Valdivia' 15:1–266

Collin SP, Hoskins RV, Partridge JC (1997) Tubular eyes of deep-sea fishes: a comparative study of retinal topography. Brain Behav Evol 50:335–357

Collin SP, Hoskins RV, Partridge JC (1998) Seven retinal specializations in the tubular eye of the deep-sea pearleye, Scopelarchus michaelsarsi: a case study in visual optimization. Brain Behav Evol 51:291–314

Contino F (1939) Das Auge des *Argyropelecus hemigymnus*. Morphologie, Bau, Entwicklung und Refraktion. Graefes Arch Ophthalmol 140:390–441

de Busserolles F, Cortesi F, Helvik JV, Davies WI, Templin RM, Sullivan RK, Michell CT, Mountford JK, Collin SP, Irigoien X, Kaartvedt S (2017) Pushing the limits of photoreception in twilight conditions: the rod-like cone retina of the deep-sea pearlsides. Sci Adv 3: eaao4709

Denton EJ (1990) Light and vision at depths greater than 200 metres. In: Herring PJ, Campbell AK, Whitfield M, Maddocks L (eds) Light and life in the sea. Cambridge University Press, pp 127–148

Dickson DH, Graves DA (1979) Fine structure of the lamprey photoreceptors and retinal pigment epithelium (*Petromyzon marinus* L.). Exp Eye Res 29:45–60

Douglas RH, Partridge JC (2011) Visual adaptations to the deep sea. In: Farrell AP (ed) Encyclopedia of fish physiology: from genome to environment, vol 1. Academic Press, pp 166–182

Douglas RH, Partridge JC, Marshall NJ (1998) The eyes of deep-sea fish I: lens pigmentation, tapeta and visual pigments. Prog Retin Eye Res 17(4):597–636

Douglas RH, Hunt DM, Bowmaker JK (2003) Spectral sensitivity tuning in the deep-sea. In: Collin SP, Marshall NJ (eds) Sensory processing in aquatic environments. Springer Verlag, pp 323–342

Dowling JE, Ripps H (1990) On the duplex nature of the skate retina. J Exp Zool 256:55–65

Fernald RD (1990) The optical system of fishes. In: Douglas RH, Djamgoz MBA (eds) The visual system of fish. Chapman & Hall, London, pp 45–61

Francke M, Kreysing M, Mack A, Engelmann J, Karl A, Makarov F, Guck J, Wolburg H, Pusch R, von der Emde G, Schuster S, Wagner H-J, Reichenbach A (2014) Grouped retinae and tapetal cups in some teleostean fisch: occurrence, structure and function. Prog Retin Eye Res 38:43–69

Franz V (1907) Bau des Eulenauges und Theorie des Teleskopauges. Biologisches Zentralblatt (Leipzig) 27:271–350

Haddock SH, Moline MA, Case JF (2010) Bioluminescence in the sea. Annu Rev Mar Sci 2:443–493

Hart NS, Coimbra JP, Collin SP, Westhoff G (2012) Photoreceptor types, visual pigments, and topographic specializations in the retinas of hydrophiid sea snakes. J Comp Neurol 520:1246–1261

Herring PJ (1990) Bioluminescent communication in the sea. In: Herring PJ, Campbell AK, Whitfield M, Maddocks L (eds) Light and life in the sea. Cambridge University Press, pp 245–264

Johnson S (2012) The optics of life. A Biologist's guide to light in nature. Princeton University Press

Kawamura S, Yokoyama S (1997) Expression of visual and nonvisual opsins in American chameleon. Vis Res 37:1867–1871

Kojima D, Okano T, Fukada Y, Shichida Y, Yoshizawa T, Ebrey TG (1992) Cone visual pigments are present in gecko rod cells. Proc Natl Acad Sci U S A 89:6841–6845

Lamb TD, Pugh EN (2004) Dark adaptation and the retinoid cycle of vision. Prog Retin Eye Res 23:307–380

Locket NA (1971) Retinal anatomy in some scopelarchid deep-sea fishes. Proc Roy Soc Lond B 178:161–184

Locket NA (1977) Adaptations to the deep-sea environment. In: Crescitelli F (ed) handbook of sensory physiology VIII/5 the visual system of vertebrates. Springer Verlag Heidelberg, New York, pp 67–192

Locket NA (2000) On the lens pad of *Benthalbella infans*, a scopelarchid deep–sea teleost. Philos Trans R Soc B Biol Sci 355:1167–1169

Ma J-X, Znoiko S, Othersen KL, Ryan JC, Das J, Isayama T, Kono M, Oprian DD, Corson DW, Cornwall MC, Cameron DA, Harosi FI, Makino CL, Crouch RK (2001) A visual pigment expressed in both rod and cone photoreceptors. Neuron 32:451–461

McDevitt DS, Brahma SK, Jeanny JC, Hicks D (1993) Presence and foveal enrichment of rhodopsin in the "all cone" retina of the American chameleon. Anat Rec 237:299–307

Meek KM, Knupp C (2015) Corneal structure and transparency. Prog Retin Eye Res 49:1–16

Munk O (1966) Ocular anatomy of some deep-sea teleosts. Dana Rep 70: 1–71

Munk O, Rasmussen JB (1993) Note on the rod-like photoreceptors in the retina of the snake *Telescopus fallax* (Fleischmann, 1831). Acta Zool 74:9–13

Partridge JC, Archer SN, van Oostrum J (1992) Single and multiple visual pigments in deep-sea fishes. J Mar Biol Assoc UK 72:113–130

Partridge JC, Douglas RH, Marshall NJ, Chung WS, Jordan TM, Wagner H-J (2014) Reflecting optics in the diverticular eye of a deep-sea barreleye fish (Rhynchohyalus natalensis). Proc R Soc Lond B Biol Sci 281:20133223

Pearcy WG, Meyer SL, Munk O (1965) A 'four-eyed' fish from the deep-sea: *Bathylychnops exilis* Cohen, 1958. Nature 207:1260–1262

Perlman I, Normann A (1998) Light adaptation and sensitivity controlling mechanisms in vertebrate photoreceptors. Prog Retin Eye Res 17: 523–563

Richardson KC, Jarett L, Finke EH (1960) Embedding in epoxy resins for ultrathin sectioning in electron microscopy. Stain Technol 35:313–323

Robison BH, Reisenbichler KR (2008) *Macropinna microstoma* and the paradox of its tubular eyes. Copeia 2008:780–784

Röll B (2000) Gecko vision—visual cells, evolution, and ecological constraints. J Neurocytol 29:471–484

Schott RK, Müller J, Yang CGY, Bhattacharyya N, Chan N, Xu M, MorrowJM GA-H, Loew ER, Tropepe V, Chang BSW (2016) Evolutionary transformation of rod photoreceptors in the all-cone retina of a diurnal garter snake. Proc Natl Acad Sci U S A 113: 356–361

Simões BF, Sampaio FL, Loew ER, Sanders KL, Fisher RN, Hart NS, Hunt DM, Partridge JC, Gower DJ (2016) Multiple rod–cone and cone–rod photoreceptor transmutations in snakes: evidence from visual opsin gene expression. Proc R Soc B Biol Sci 283:20152624

Steinberg RH, Reid M, Lacy PL (1973) The distribution of rods and cones in the retina of the cat (*Felis domesticus*). J Comp Neurol 148:229–248

Turner JR, White EM, Collins MA, Partridge JC, Douglas RH (2009) Vision in lanternfish (Myctophidae): adaptations for viewing bioluminescence in the deep-sea. Deep-Sea Res I Oceanogr Res Pap 56: 1003–1017

Underwood G (1968) Some suggestions concerning vertebrate visual cells. Vis Res 8:483–488

Wagner H-J (2007) Bipolar cells in the "grouped retina" of the elephantnose fish (*Gnathonemus petersii*). Vis Neurosci 24:355–362

Wagner H-J, Fröhlich E, Negishi K, Collin SP (1998) The eyes of deep-sea fish II. Functional morphology of the retina. Prog Retin Eye Res 17:637–685

Wagner H-J, Douglas RH, Frank TM, Roberts NW, Partridge JC (2009) A novel vertebrate eye using both refractive and reflective optics. Curr Biol 19:108–114

Walls GL (1934) The reptilian retina. I. A new concept of visual cell evolution. Am J Ophthalmol 17:892–915

Walls GL (1942) The vertebrate eye and its adaptive radiation. Fafner Publishing Company, New York

Warrant EJ, Locket A (2004) Vision in the deep-sea. Biol Rev 79:671–712

Weale RA (1955) Binocular vision and deep-sea fish. Nature 175:996

Widder EA (1999) Bioluminescence. In: Archer SN, Djamgoz MBA, Loew ER, Partridge JC, Vallerga S (eds) Adaptive mechanisms in the ecology of vision. Kluwer Academic Publishers, Dordrecht, pp 555–581

Yokoyama S, Blow NS (2001) Molecular evolution of the cone visual pigments in the pure rod-retina of the nocturnal gecko, *Gekko gekko*. Gene 276:117–125